Differential effects on neuromuscular physiology between *Sod1* loss-of-function mutation and paraquat-induced oxidative stress in *Drosophila*

Atsushi Ueda[1], Atulya Iyengar[1,2§] and Chun-Fang Wu[1,2]

[1]Dept. Biology, University of Iowa

[2]Iowa Neuroscience Institute, University of Iowa

[§]To whom correspondence should be addressed: atulya-iyengar@uiowa.edu

Abstract

Oxidative stress is thought to be a major contributor to aging processes. Here, we report differential effects on neurotransmission caused by loss-of-function mutations of *Superoxide dismutase 1* (*Sod1*) and by paraquat (PQ) feeding in *Drosophila*. We demonstrated alterations in *Sod1* mutants; the larval neuromuscular junction displayed supernumerary discharges and the adult giant-fiber escape pathway showed increased latency and poor response to repetitive high-frequency stimulation. Even though the concentrations used led to motor coordination defects and lethality, PQ feeding failed to reproduce such performance deficits in these larval and adult preparations, indicating mechanistic distinctions between these genetic and pharmacological manipulations of oxidative stress.

Supernumerary EJPs

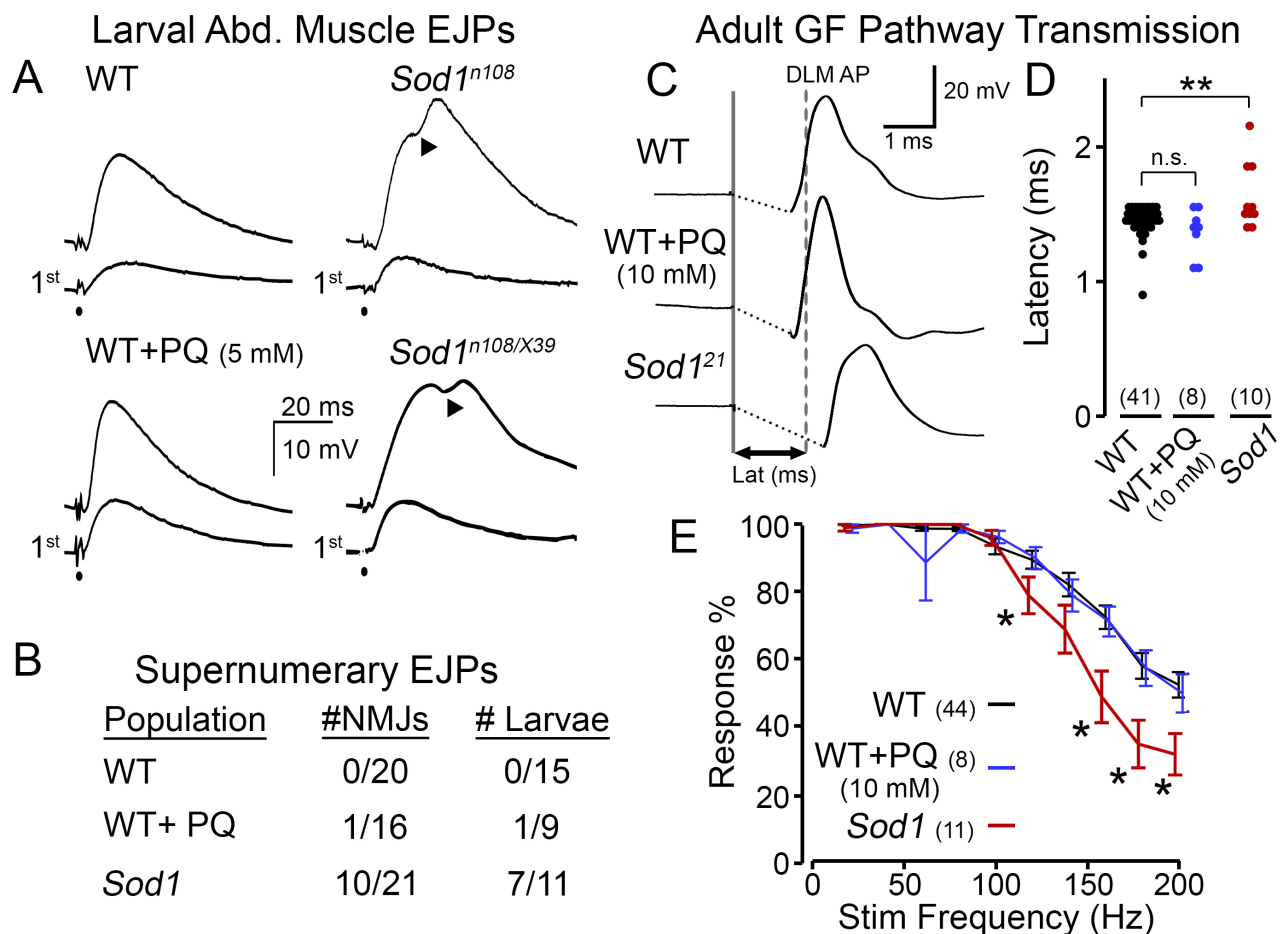| Population	#NMJs	# Larvae
WT	0/20	0/15
WT+ PQ	1/16	1/9
Sod1	10/21	7/11

Figure 1. Comparison of *Sod1* mutational and paraquat (PQ) pharmacological effects on electrophysiological properties of the *Drosophila* motor system: (A, B) Synaptic transmission at neuromuscular junctions (NMJs) of abdominal body-wall muscles in 3rd instar larvae. (A) Excitatory junctional potentials (EJPs) triggered by 0.1-ms motor axon stimulation. Upon repetitive nerve stimulation (15 Hz) supernumerary EJPs occur at NMJs in *Sod1* mutants (arrowheads). The initial EJPs ("1st") were not significantly different among WT control, PQ-fed WT, and *Sod1* mutant larvae. However, subsequent nerve stimulation induced supernumerary EJPs ('▲' indicate humps in EJPs) in *Sod1* larvae, but not in WT control or PQ-fed WT (see traces above the "1st" EJPs). (B) Proportion of NMJs and larvae (in WT, PQ-fed WT, and mutant (*Sod1[n108 or n108/X39]*) samples) displaying supernumerary EJPs. PQ concentration in food was 5 - 10 mM. Experiments were performed in HL3.1 saline (Feng *et al.*, 2004) containing low levels of Ca^{2+} (0.1 - 0.2 mM). (C-E) Performance of the giant fiber (GF) jump-and-flight escape circuit in adult flies. Ages for WT flies and *Sod1* mutants were

selected to be comparable mortality (< 5%, WT 7-8 d., *Sod1* 2-3 d., see Iyengar *et al.*, 2020 for details). (C) Electrical stimulation across the head directly activated GF pathway leading to flight muscle spikes monitored in dorsal longitudinal muscles (DLMs). The latency to spiking was measured as the duration between stimulus (solid line) and the DLM depolarization reaching its half-maximal amplitude (dashed line for WT). Stimulus artifacts have been removed for clarity. Note the retarded response in *Sod1* mutant. (D) Scatterplot of the GF transmission latency for WT, PQ-fed WT and *Sod1* mutants. Data points indicate latency from individual flies. (E) Frequency response of the GF pathway. Stimulus trains were delivered at progressively higher frequencies (20 – 200 Hz, see Methods), and the response rate was recorded. Note that *Sod1* mutants display a relatively poor ability to follow high-frequency stimulation compared to PQ- and control-fed WT flies. For (D-E), numbers of flies studied are indicated in parenthesis.

Description

Free radicals, such as the superoxide anion (O_2^-) impart oxidative stress upon an animal and are thought to be a major contributing factor to age-related changes in the nervous system (Finkel & Holbrook, 2000; Harman, 1956; Harman, 1981). In eukaryotes, the cytosolic enzyme Cu^{2+}/Zn^{2+} Superoxide Dismutase (in *Drosophila* encoded by *Sod1*, originally *cSOD*, Campbell *et al.*, 1986) is an important free radical scavenger that converts superoxide into hydrogen peroxide. *Drosophila Sod1* loss-of-function mutants exhibit elevated levels of reactive oxygen species (ROS) combined with a drastically shortened adult lifespan (median ~11 d. vs 50 d. for wild-type flies at 25 °C, Phillips *et al.*, 1989) and reduced locomotor ability in larvae (Şahin *et al.*, 2017) and adults (Ruan & Wu, 2008). Coupled with these longevity and behavioral phenotypes, several neuromuscular deficits have recently been identified in *Sod1* loss-of-function mutants including deranged nerve and synapse morphology in larvae (Milton *et al.*, 2011) and adults (Agudelo *et al.*, 2020; Şahin *et al.*, 2017), as well as disrupted neurotransmission along the giant-fiber (GF) jump-and-flight escape circuit (Iyengar *et al.*, 2020; Iyengar, 2016; Ruan, 2008). Given the striking phenotypes, a question that arises is: To what extent the straightforward assumption holds that aspects of the *Sod1* phenotypes can be recapitulated by pharmacologically induced oxidative stress?

Here, we compare neuromuscular physiology in *Sod1* loss-of-function ('null') mutants to wild-type (WT) flies with elevated oxidative stress levels induced by paraquat (PQ) feeding. A widely used herbicide, PQ is a well-studied drug often utilized experimentally to generate superoxide anions and induce oxidative stress in *Drosophila* (Parkes *et al.*, 1993; Shukla *et al.*, 2014). We examined synaptic transmission at the abdominal neuromuscular junction (NMJ) of 3rd instar *Sod1* larvae to WT larvae fed on PQ-containing medium from egg hatching. In adults, we compared the performance of the GF escape pathway (Engel & Wu, 1992) in *Sod1* mutants to PQ-fed WT flies. The PQ feeding concentrations chosen for this study (5 or 10 mM throughout the larval stage; and 10 mM in adults for 4 d) were reported to induce lethality and behavioral abnormalities in WT flies within a 3 – 7 d window (Arking *et al.*, 1991; Jahromi *et al.*, 2013). Over this period, we indeed observed a marked loss of motor coordination. Flies often "stumbled" while walking and occasionally exhibited wing-buzzes upon gentle "tapping" of the vial. The PQ concentrations selected for exposing larvae throughout their development was near lethality levels, beyond which few larvae survived. Nevertheless, our neurophysiological findings reveal that PQ-fed WT individuals clearly do not replicate all *Sod1* phenotypes in both larval and adult physiological recordings.

At the larval NMJ, we found *Sod1* mutant larvae displayed a striking phenotype which was absent in WT counterparts (Figure 1A). Although an initial nerve stimulation produced similar excitatory junctional potentials (EJPs, analogous to EPSPs) in WT and *Sod1* larvae (lower traces), after repetitive stimulation (at ~15 Hz, upper traces), we observed extra 'humps' in the *Sod1* waveforms indicative of supernumerary EJPs (representative EJPs from a homozygous *Sod1^{n108}* and hetero-allelic *Sod1^{n108}/Sod1^{X39}* individuals are shown). These abnormal events indicate the stimuli recruit secondary action potentials in the motor nerve (Ueda & Wu, 2009) and suggest a form of nerve hyperexcitability in *Sod1* mutants. In contrast, PQ-fed WT flies displayed EJPs that were remarkably similar to control diet-fed counterparts in terms of shape and amplitude. Indeed, across the population of larvae, extra 'humps' in the EJP waveform were commonly observed in *Sod1* larvae but were exceedingly rare in PQ-fed WT or control-fed WT flies (Figure 1B).

To compare the effects of PQ feeding and *Sod1* mutations on adult nervous system function, we examined stimulus-response relationships of the GF pathway. In this circuit, established visual and mechanosensory inputs trigger spiking in the GF neuron in response to visual looming or air pressure stimuli (Card & Dickinson, 2008; Lehnert *et al.*, 2013; Mu *et al.*, 2014; Trimarchi & Schneiderman, 1995). The descending GF axons project directly to the tergotrochanteral (TTM, 'jump muscle') motor unit and indirectly via the peripherally synapsing interneuron (PSI) to the dorsal longitudinal muscle (DLM, 'flight muscle') motor unit (Gorczyca & Hall, 1984; King & Wyman, 1980). Direct electrical stimulation of the GF neuron triggers an action potential in the DLM with a stereotypic latency in WT flies (~1.4 ms, Figure 1C), known as 'short-latency' responses (Engel & Wu, 1996). Consistent with previous observations (Iyengar *et al.*, 2020), we found *Sod1* flies displayed an overall increase in latency with a wider variability compared to WT counterparts (Figure 1C-D). However, PQ-fed WT flies did not show such retarded responses; instead latencies displayed were remarkably similar to control WT individuals. We also examined the ability of the GF pathway to follow trains of high-frequency

stimulation (20 – 200 Hz) in PQ-fed flies and *Sod1* mutants (Figure 1E). At stimulation frequencies higher than 100 Hz, we found *Sod1* displayed a progressively worse ability to follow stimulation compared to WT counterparts (largely consistent with observations using a twin-pulse refractory protocol, c.f. Iyengar *et al.*, 2020). However, across all frequencies, PQ-fed WT flies displayed a similar response rate compared to control diet-fed individuals.

Our observations at the larval NMJ and along the GF pathway in adults reveal clear and consistent defects in neurotransmission among *Sod1* loss-of-function mutants. It should be noted that mutant flies harboring an amyotrophic lateral sclerosis (ALS)-associated allele (*G85R*) has been reported to display a collection of neuromuscular defects, including NMJ overgrowth and moderately increased spontaneous miniature EJPs, which can be further compared with PQ-feeding effects in future studies (Held *et al.*, 2019). The *Sod1* alleles we studied, i.e. $Sod1^{n108}$, $Sod1^{X39}$ and $Sod1^{21}$, were independently isolated (Phillips *et al.*, 1989; Şahin *et al.*, 2017). Thus, it is most likely *Sod1* disruption, rather than contributions from secondary 'background' mutations, gives rise to the phenotypes. We observed poor motor coordination and lethality, indicating our PQ-feeding indeed produced effects consistent with previous reports (Arking *et al.*, 1991). Notably, even though the larval NMJ and adult GF pathway are remarkably robust systems, studies from our group and others have demonstrated clear electrophysiological alterations in *Sod1* loss-of-function (this study; see also: Watson, *et al.*, 2008, Iyengar, *et al.*, 2020). In contrast, pharmacological manipulation of oxidative stress levels with standard PQ-feeding protocol failed to recapitulate *Sod1* mutant phenotypes, suggesting the neuromuscular deficits in *Sod1* flies described here do not arise by a simple overall elevation of superoxide levels. One possible contributing factor is altered regulation of superoxide anions in specific cell types or subcellular compartments leading to the complexity or diversity of *Sod1* mutant phenotypes. Alternatively, mutations in *Sod1* or PQ-exposure can induce different patterns of downstream adjustments involving altered activity of other redox enzymes (Missirlis *et al.*, 2003) and of different 2nd messenger signaling pathways such as BMP signaling (Berke *et al.*, 2013; Held *et al.*, 2019), Nrf2/KEAP1 and/or NF-KB, (Sies *et al.*, 2017; Wang *et al.*, 2018).

Methods
Request a detailed protocol

Fly Stocks and Drug Feeding

The *Sod1* (originally *cSOD*, Campbell *et al.*, 1986; also known as *Sod*, Ruan & Wu, 2008) hypomorphic/null mutant alleles examined included: $Sod1^{n108}$ (also known as $Sod1^{n1}$) [FBal0015933]; $Sod1^{X39}$ [FBal0030258] (Campbell *et al.*, 1986; Phillips *et al.*, 1989); and $Sod1^{21}$ [FBal0343866] (Şahin *et al.*, 2017). We studied homozygous *n108*, and *21* individuals; however, we examined the hetero-allelic *n108/X39* combination due to the poor viability of homozygous *X39* flies (Ruan & Wu, 2008). Phenotypes among the *Sod1* alleles were remarkably similar. Therefore, the data was pooled for statistical analyses (Figure 1B, D & E). The WT strain was *Canton-Special*. For adult experiments, we studied WT and *Sod1* populations before significant age-dependent mortality (< 1% and 5% mortality, 7-8 d for WT and 2-3 d *Sod1*). For detailed characterization of the age-dependence of GF performance in *Sod1* and WT flies, see Iyengar *et al.* (2020).

Flies were reared on Frankel & Brosseau (1968) cornmeal-based media (see Kasuya *et al.*, 2019) at room temperature (23 °C). To make PQ-laced media, measured amounts of paraquat (Sigma #856177) and Blue #1 dye (to indicate mixing, flavorsandcolor.com, Diamond Bar, CA) were added to melted fly media to achieve final concentrations of 5 or 10 mM PQ and 25 µg/ml dye. For larval feeding experiments, larvae were reared on PQ media (5 mM or 10 mM) from egg hatching until the post-feeding 3rd instar stage. Adults were aged to 3 – 4 d. and were then fed with PQ-containing (10 mM) medium for 4 d and used for recording.

Larval Neuromuscular Electrophysiology

Neuromuscular recordings from post-feeding 3rd instar larvae are described in (Ueda & Wu, 2006, 2009). Dissections were performed in Ca^{2+}-free HL3 saline (Stewart *et al.*, 1994). Excitatory junction potentials (EJPs) were recorded from abdominal muscles in HL3.1 saline (Feng *et al.*, 2004) containing relatively low Ca^{2+} levels (0.1 or 0.2 mM). To evoke nerve action potentials and EJPs, the segmental nerve was severed form the ventral ganglion and stimulated through the cut-end with a suction electrode (~10-µm inner diameter). The stimulation pulse train (0.1 ms stimuli delivered at 15 Hz for 50 s) was generated from a Grass S88 stimulator (West Warwick, RI) through a custom-made isolation unit. The stimulation voltage was adjusted to be double the EJP threshold value to ensure motor axon stimulation. To record EJPs, a glass intracellular microelectrode filled with 3 M KCl (~ 60 MΩ resistance) was inserted in the abdominal muscle # 6/7 (Crossley, 1979). Signals were recorded by a DC amplifier (model M701, WPI, Sarasota, FL and an additional custom-built amplifier) and digitized using a data acquisition card (USB 6212, National Instruments, Austin TX) and pClamp5 (Molecular Devices, Burlingame, California, USA) controlled by a PC.

Adult Giant-Fiber Physiology

Examination of the giant-fiber pathway physiology were performed in tethered flies (see Engel and Wu (1992); Iyengar and Wu (2014) for details). Flies were anesthetized on ice, affixed to a tungsten pin with cyanoacrylate glue, and given

~30 min to recover. To record spiking from the DLM, an electrolytically sharpened tungsten electrode was inserted into the attachment site of the dorsal-most fiber (#45, see Miller, 1950). A similarly constructed electrode was inserted into the abdomen as reference. Electrical activity was picked-up by an AC amplifier (gain: 100x, bandwidth: 10 – 10,000 Hz, AM systems Model 1800) and digitized by data acquisition card (USB 6212, National Instruments) controlled by a PC running LabVIEW (2018, National Instruments).

Electrical stimulation to activate the GF pathway was delivered by an isolated pulse stimulator (AM systems Model 2100) via sharpened tungsten electrodes inserted in each cornea. Stimuli consisted of brief pulses (0.1 ms duration, 30 V amplitude) which reliably activated the GF neuron and downstream elements ('short-latency responses' in Engel & Wu, 1996; Iyengar *et al.*, 2020). The GF latency (Figure 1D) was determined as the interval between stimulation and the DLM spike reaching its half-maximum height. The frequency following ability of the GF pathway was determined by delivering trains of 10 pulses at increasing frequencies (20 Hz – 200 Hz in 20 Hz increments) with a 5-s interval between trains. For each pulse train, the number of DLM responses divided by number of stimuli was reported.

Statistical Analysis

All statistical analysis was done in MATLAB (r2020b, MathWorks). Kruskal-Wallis non-parametric ANOVA tests (with Holm-Bonferroni corrected rank-sum *post hoc* analysis) were employed to establish statistical significance in Figure 1D and E. * $p < 0.05$, and ** $p < 0.01$.

References

Agudelo A, St Amand V, Grissom L, Lafond D, Achilli T, Sahin A, Reenan R, Stilwell G. 2020. Age-dependent degeneration of an identified adult leg motor neuron in a *Drosophila* SOD1 model of ALS. Biol Open 9: . PMID: 32994185.

Arking R, Buck S, Berrios A, Dwyer S, Baker GT 3rd. 1991. Elevated paraquat resistance can be used as a bioassay for longevity in a genetically based long-lived strain of Drosophila. Dev Genet 12: 362-70. PMID: 1806332.

Berke B, Wittnam J, McNeill E, Van Vactor DL, Keshishian H. 2013. Retrograde BMP signaling at the synapse: a permissive signal for synapse maturation and activity-dependent plasticity. J Neurosci 33: 17937-50. PMID: 24198381.

Campbell SD, Hilliker AJ, Phillips JP. 1986. Cytogenetic analysis of the cSOD microregion in Drosophila melanogaster. Genetics 112: 205-15. PMID: 11933981.

Card G, Dickinson MH. 2008. Visually mediated motor planning in the escape response of Drosophila. Curr Biol 18: 1300-7. PMID: 18760606.

Crossley, A. 1979. The morphology and development of the *Drosophila* muscular system. In M. W. Ashburner, T (Ed.), *The genetics and biology of Drosophila* (pp. 400 - 560). New York, NY USA: Academic Press.

Engel JE, Wu CF. 1992. Interactions of membrane excitability mutations affecting potassium and sodium currents in the flight and giant fiber escape systems of Drosophila. J Comp Physiol A 171: 93-104. PMID: 1328625.

Engel JE, Wu CF. 1996. Altered habituation of an identified escape circuit in Drosophila memory mutants. J Neurosci 16: 3486-99. PMID: 8627381.

Feng Y, Ueda A, Wu CF. 2004. A modified minimal hemolymph-like solution, HL3.1, for physiological recordings at the neuromuscular junctions of normal and mutant Drosophila larvae. J Neurogenet 18: 377-402. PMID: 15763995.

Finkel T, Holbrook NJ. 2000. Oxidants, oxidative stress and the biology of ageing. Nature 408: 239-47. PMID: 11089981.

Frankel AWK, Brosseau GE. 1968. Drosophila medium that does not require dried yeast. Drosophila Information Service 43:184.

Gorczyca M, Hall JC. 1984. Identification of a cholinergic synapse in the giant fiber pathway of Drosophila using conditional mutations of acetylcholine synthesis. J Neurogenet 1: 289-313. PMID: 6443123.

Harman D. 1956. Aging: a theory based on free radical and radiation chemistry. J Gerontol 11: 298-300. DOI: 10.1101/2020.08.19.257832 | PMID: 13332224.

Harman D. 1981. The aging process. Proc Natl Acad Sci U S A 78: 7124-8. PMID: 6947277.

Held A, Major P, Sahin A, Reenan RA, Lipscombe D, Wharton KA. 2019. Circuit Dysfunction in *SOD1-ALS* Model First Detected in Sensory Feedback Prior to Motor Neuron Degeneration Is Alleviated by BMP Signaling. J Neurosci 39: 2347-2364. PMID: 30659087.

Iyengar, A., Ruan, H., & Wu, C.-F. 2020. Distinct aging-vulnerable trajectories of motor circuit functions in oxidation- and temperature-stressed Drosophila. *bioRxiv*, DOI: 10.1101/2020.08.19.257832

Iyengar A, Wu CF. 2014. Flight and seizure motor patterns in Drosophila mutants: simultaneous acoustic and electrophysiological recordings of wing beats and flight muscle activity. J Neurogenet 28: 316-28. PMID: 25159538.

Iyengar, A. S. R. 2016. *An integrative analysis of neuronal hyperexcitability, central pattern generation and aberrant motor behavior through the lens of Drosophila neurogenetics.* (PhD). University of Iowa, Iowa City. DOI: 10.17077/etd.kjtqmy8x

Jahromi SR, Haddadi M, Shivanandappa T, Ramesh SR. 2013. Neuroprotective effect of Decalepis hamiltonii in paraquat-induced neurotoxicity in Drosophila melanogaster: biochemical and behavioral evidences. Neurochem Res 38: 2616-24. PMID: 24173775.

Kasuya J, Iyengar A, Chen HL, Lansdon P, Wu CF, Kitamoto T. 2019. Milk-whey diet substantially suppresses seizure-like phenotypes of *para^Shu^*, a *Drosophila* voltage-gated sodium channel mutant. J Neurogenet 33: 164-178. PMID: 31096839.

King DG, Wyman RJ. 1980. Anatomy of the giant fibre pathway in Drosophila. I. Three thoracic components of the pathway. J Neurocytol 9: 753-70. PMID: 6782199.

Lehnert BP, Baker AE, Gaudry Q, Chiang AS, Wilson RI. 2013. Distinct roles of TRP channels in auditory transduction and amplification in Drosophila. Neuron 77: 115-28. PMID: 23312520.

Miller A. 1950. The internal anatomy and histology of the imago of Drosophila melanogaster. (pp. 420 - 534). in Demeric M. (Ed.) Biology of Drosophila. John Wiley & Sons, Inc. New York

Milton VJ, Jarrett HE, Gowers K, Chalak S, Briggs L, Robinson IM, Sweeney ST. 2011. Oxidative stress induces overgrowth of the Drosophila neuromuscular junction. Proc Natl Acad Sci U S A 108: 17521-6. PMID: 21987827.

Missirlis F, Hu J, Kirby K, Hilliker AJ, Rouault TA, Phillips JP. 2003. Compartment-specific protection of iron-sulfur proteins by superoxide dismutase. J Biol Chem 278: 47365-9. PMID: 12972424.

Mu L, Bacon JP, Ito K, Strausfeld NJ. 2014. Responses of Drosophila giant descending neurons to visual and mechanical stimuli. J Exp Biol 217: 2121-9. PMID: 24675562.

Parkes TL, Hilliker AJ, Phillips JP. 1993. Genetic and biochemical analysis of glutathione-S-transferase in the oxygen defense system of Drosophila melanogaster. Genome 36: 1007-14. PMID: 8112568.

Phillips JP, Campbell SD, Michaud D, Charbonneau M, Hilliker AJ. 1989. Null mutation of copper/zinc superoxide dismutase in Drosophila confers hypersensitivity to paraquat and reduced longevity. Proc Natl Acad Sci U S A 86: 2761-5. PMID: 2539600.

Ruan, H. 2008. *On Drosophila aging: Lifespan plasticity, social-behavioral influences, and neurophysiological indices* (PhD): The University of Iowa, Iowa CIty, IA.

Ruan H, Wu CF. 2008. Social interaction-mediated lifespan extension of Drosophila Cu/Zn superoxide dismutase mutants. Proc Natl Acad Sci U S A 105: 7506-10. PMID: 18508973.

Şahin A, Held A, Bredvik K, Major P, Achilli TM, Kerson AG, Wharton K, Stilwell G, Reenan R. 2017. Human SOD1 ALS Mutations in a Drosophila Knock-In Model Cause Severe Phenotypes and Reveal Dosage-Sensitive Gain- and Loss-of-Function Components. Genetics 205: 707-723. PMID: 27974499.

Shukla AK, Pragya P, Chaouhan HS, Patel DK, Abdin MZ, Kar Chowdhuri D. 2014. Mutation in Drosophila methuselah resists paraquat induced Parkinson-like phenotypes. Neurobiol Aging 35: 2419.e1-2419.e16. PMID: 24819147.

Sies H, Berndt C, Jones DP. 2017. Oxidative Stress. Annu Rev Biochem 86: 715-748. PMID: 28441057.

Stewart BA, Atwood HL, Renger JJ, Wang J, Wu CF. 1994. Improved stability of Drosophila larval neuromuscular preparations in haemolymph-like physiological solutions. J Comp Physiol A 175: 179-91. PMID: 8071894.

Trimarchi JR, Schneiderman AM. 1995. Flight initiations in Drosophila melanogaster are mediated by several distinct motor patterns. J Comp Physiol A 176: 355-64. PMID: 7707271.

Ueda A, Wu CF. 2006. Distinct frequency-dependent regulation of nerve terminal excitability and synaptic transmission by IA and IK potassium channels revealed by Drosophila Shaker and Shab mutations. J Neurosci 26: 6238-48. PMID: 16763031.

Ueda A, Wu CF. 2009. Effects of social isolation on neuromuscular excitability and aggressive behaviors in Drosophila: altered responses by Hk and gsts1, two mutations implicated in redox regulation. J Neurogenet 23: 378-94. PMID: 19863269.

Wang Y, Branicky R, Noë A, Hekimi S. 2018. Superoxide dismutases: Dual roles in controlling ROS damage and regulating ROS signaling. J Cell Biol 217: 1915-1928. PMID: 29669742.

Watson MR, Lagow RD, Xu K, Zhang B, Bonini NM. 2008. A drosophila model for amyotrophic lateral sclerosis reveals motor neuron damage by human SOD1. J Biol Chem 283: 24972-81. PMID: 18596033.